

Nanoscale

Accepted Manuscript



This is an *Accepted Manuscript*, which has been through the Royal Society of Chemistry peer review process and has been accepted for publication.

Accepted Manuscripts are published online shortly after acceptance, before technical editing, formatting and proof reading. Using this free service, authors can make their results available to the community, in citable form, before we publish the edited article. We will replace this *Accepted Manuscript* with the edited and formatted *Advance Article* as soon as it is available.

You can find more information about *Accepted Manuscripts* in the [Information for Authors](#).

Please note that technical editing may introduce minor changes to the text and/or graphics, which may alter content. The journal's standard [Terms & Conditions](#) and the [Ethical guidelines](#) still apply. In no event shall the Royal Society of Chemistry be held responsible for any errors or omissions in this *Accepted Manuscript* or any consequences arising from the use of any information it contains.

Superabsorption of Light by Multilayer Nanowires

Ali Mirzaei,* Ilya V. Shadrivov, Andrey E. Miroshnichenko and Yuri S. Kivshar

Received Xth XXXXXXXXXXXX 20XX, Accepted Xth XXXXXXXXXXXX 20XX

First published on the web Xth XXXXXXXXXXXX 200X

DOI: 10.1039/b000000x

We suggest a new strategy for tailoring and enhancing the absorption of light by multilayered nanowires. We use the multipole expansion method and experimental data for dielectric and plasmonic materials and demonstrate that the absorption for one of the polarizations can be substantially enhanced due to an overlap of different resonant modes in nanowires. We show that our approach can be employed for a design of multiband tunable optical absorption across a wide spectral range for both TE and TM polarizations.

Light absorption and its enhancement in nanostructures, including spherical and cylindrical geometries, is fundamentally important,^{1–3} and can be used in various applications, including light detection at the nanoscale and selective color absorption. In biology and medicine, the absorption of infrared light by noninvasive cell-tracking nanoparticles leads to the improvements in the cancer diagnostics techniques and detection of infectious microorganisms.^{4–8} In physics, quantum-engineered superabsorption is used for improving optical sensors and light harvesting technologies.⁹ Solar cells and thermophotovoltaic devices also benefit from larger light absorption which significantly improves their efficiency.^{10–14}

To achieve higher absorption, various strategies and geometrical designs have been analyzed. Perfect absorbers^{15–20}, omnidirectional absorption by reflectionless impedance matching in periodic arrays and nanoscale gratings^{21–23}, and spatial trapping of resonances in semiconductors to improve the solar energy conversion²⁴ have been studied. Wide-band thin super-absorption, using hyperbolic metamaterials^{25–27} and black-bodies^{28–30} using plasmonic resonances are also introduced.

One important technique to obtain higher absorption by nanostructures is spectrally overlapping several absorption resonances, for example by using Mie and leaky/guided modes in nanowires,³¹ or by overlapping the resonances from different polarizations^{32,33}. Enhancement of the absorption for one polarization (either TE or TM) has been also suggested by utilizing two resonant modes³². However, to the best of our knowledge, the strategy for overlapping multiple

Nonlinear Physics Centre, Australian National University, Acton, ACT, 2601, Australia. Fax: +61 2 6125 8588; Tel: +61 2 6125 4983; E-mail: ali.mirzaei@anu.edu.au

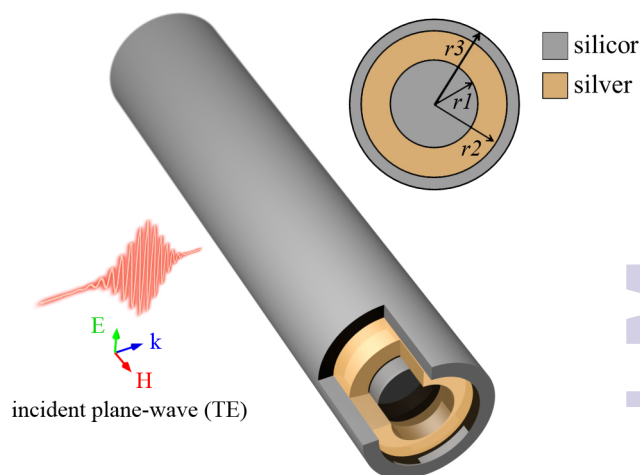


Fig. 1 Schematics of the problem: electromagnetic plane wave is incident on a multilayer nanowire whose layers are made of silicon and silver.

resonances and its tunability is not comprehensively studied in neither plasmonic nor all-dielectric structures.

In this Letter we introduce a highly tunable approach for overlapping various absorption resonances of different modes, in either TE or TM polarizations. By using experimental data for material parameters^{34,35}, we design and analyze superabsorption by multilayer nanowires with the total absorbed energy being substantially larger than that achieved in homogeneous structures of the same size. Herein, by adding one plasmonic (silver) or dielectric (aluminium arsenide) shell to a silicon nanowire, we demonstrate an overlap of up to four different absorption resonances of the same polarization. We demonstrate that, the substantially enhanced absorption occurs mostly in the semiconductor layers which is important for photovoltaics and solar-cell applications.

The absorption cross-section (ACS) in two-dimensional case is calculated as $\sigma^a = P^{abs}/I_0$, where P^{abs} is the absorbed power and I_0 is the incident power density, both per unit length. Absorption by nanowires can be studied in cylindrical coordinates, and ACS can be presented as a superposition of absorption contributions from different cylindrical modes. This decomposition can generally be presented as

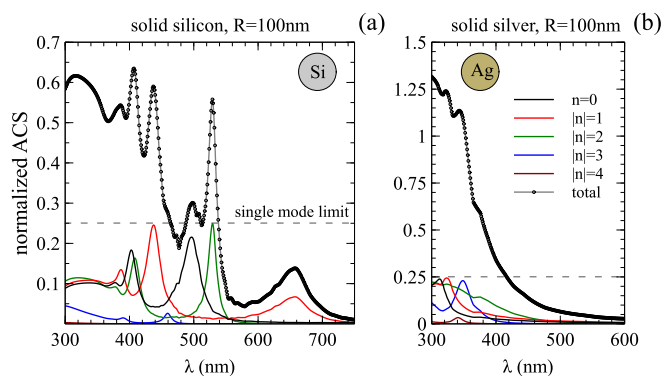


Fig. 2 Spectrum of the total absorption cross-section for TE polarization, as well as contributions of individual modes for solid (a) silicon and (b) silver nanowires. The figure shows non-overlapped absorption resonances of different modes in solid dielectric and their concentration close to the plasmonic resonance wavelength in metallic nanowires.

$\sigma^a = \sum_{n=-\infty}^{+\infty} \sigma_n^a$, where σ_n^a is a single mode ACS and n is the mode number.³⁶ The spectral behavior of absorption of each mode is a function of the size and material parameters of the nanowire.

In a single nanowire, mode degeneracy of the positive and negative orders appears due to the azimuthal symmetry. Their contribution to the absorption is equal across the spectrum, except for $n = 0$ mode. The absorption spectrum also depends on material parameters. In solid metallic nanowires the absorption is considerable only close to the plasmonic resonance frequency and relatively small everywhere else. In solid dielectric nanowires, several resonances exist, but they are well spaced in the frequency domain, so that the overlap between them is not substantial. To overcome these restrictions of enhancing the absorption, here we introduce multimode absorption approach, aiming at a design of structures that have several resonances co-existing at a selected frequency. To achieve this, we engineer multilayer nanostructures whose absorption is enhanced far beyond the single-mode limit. We use a genetic optimization algorithm^{37–39} (GA) and define a fitness function for a three-layer nanowire as $F(r_1, r_2, r_3) = \max\{ACS(\lambda_{opt}, r_1, r_2, r_3)\}$, where λ_{opt} indicates the operating wavelength. This optimization process allows to design the enhanced absorption at any selected wavelength, or even simultaneously for several frequency bands. The details of the developed GA, definition of genes and chromosomes, and other details can be found in previously published works³⁷.

From the energy conservation for non-radiating modes, the σ^a can be written as $\sigma^a = \sigma^e - \sigma^s$, where σ^e and σ^s are extinction and scattering cross-sections, respectively. We consider an infinite multilayer nanowire shown schematically in

Fig. 1. An incident plane wave is assumed to propagate in the x direction. For TE polarization (the electric field is perpendicular to the cylinder axis), the magnetic field can be written as $\mathbf{H}^{inc} = \hat{\mathbf{a}}_z H_0 e^{-i\omega t + i2\pi\lambda^{-1}r\cos(\varphi)}$, where φ is the polar angle in the cylindrical coordinates. By using the multipole expansion method to describe the interaction of light with a nanowire,^{40,41} the total field can be presented as

$$H_z^l = H_0 e^{-i\omega t} \sum_{n=-\infty}^{+\infty} e^{in(\varphi + \frac{\pi}{2})} \left[\tau_n^l J_n(\beta_l r) + \rho_n^l H_n^{(1)}(\beta_l r) \right], \quad (1)$$

where $\beta_l = 2\pi\lambda^{-1}[\epsilon_l(\lambda)]^{\frac{1}{2}}$, H_0 is the amplitude of the incident plane wave, J_n and $H_n^{(1)}$ are the n -th order Bessel and Hankel functions of the first kind, respectively; n is the mode number, l is the layer number, L is total number of layers, and index $L + 1$ corresponds to the surrounding medium, $\epsilon_l(\lambda)$ is the dielectric constant of the l -th layer at wavelength λ . Amplitudes of partial waves in the l -th layer τ_n^l and ρ_n^l are found by solving the boundary condition equations for the continuity of the tangential components H_z and E_φ . Additionally, we put $\rho_n^1 = 0$ to avoid singularity of Hankel functions in the centre of the nanowire, and $\tau_n^{L+1} = 1$ for each n to describe the incident plane wave in cylindrical coordinates. For TM polarization an expression similar to Eq. (1) can be written for E^l , and the expansion coefficients can be found by satisfying the boundary conditions for the tangential components of fields E_z and H_φ .

Here we mention that small-size plasmonic nanoparticles may have dielectric constants quite different from those of bulk materials.⁴² When the size of a nanowire becomes comparable with the electron mean-free path, the collision frequency should be modified. The small-size effect is analytically described for the Drude model of metal permittivity, however in present work we use experimental data that deviates from the Drude model, which is given by $\epsilon = \epsilon_\infty - \omega_p^2 / (\omega^2 + i\gamma\omega)$, where for silver $\epsilon_\infty = 4.96$.³⁴ In order to account for the small-size effects while using the experimentally measured material parameters, we perform the following steps. For each frequency, we use complex values of experimentally measured permittivity to find plasma frequency ω_p and collision frequency γ , so that the Drude formula gives correct permittivity of a bulk material at this frequency. Then we modify γ , making the following replacement: $\gamma_{small-particle} = \gamma_{bulk} + V_f/D$, where $V_f = 1.388 \cdot 10^6$ m/s is the Fermi velocity in silver and D is the characteristic size of a metallic structure. Finally, by using $\gamma_{small-particle}$ in the Drude formula, we obtain the real and imaginary parts of the corrected dielectric constant.^{38,42}

Now by solving the boundary condition equations and obtaining the expansion coefficients, the σ^s which for infinite cylindrical structures is defined as the ratio of the scattered power per unit length to the incident energy flux per unit

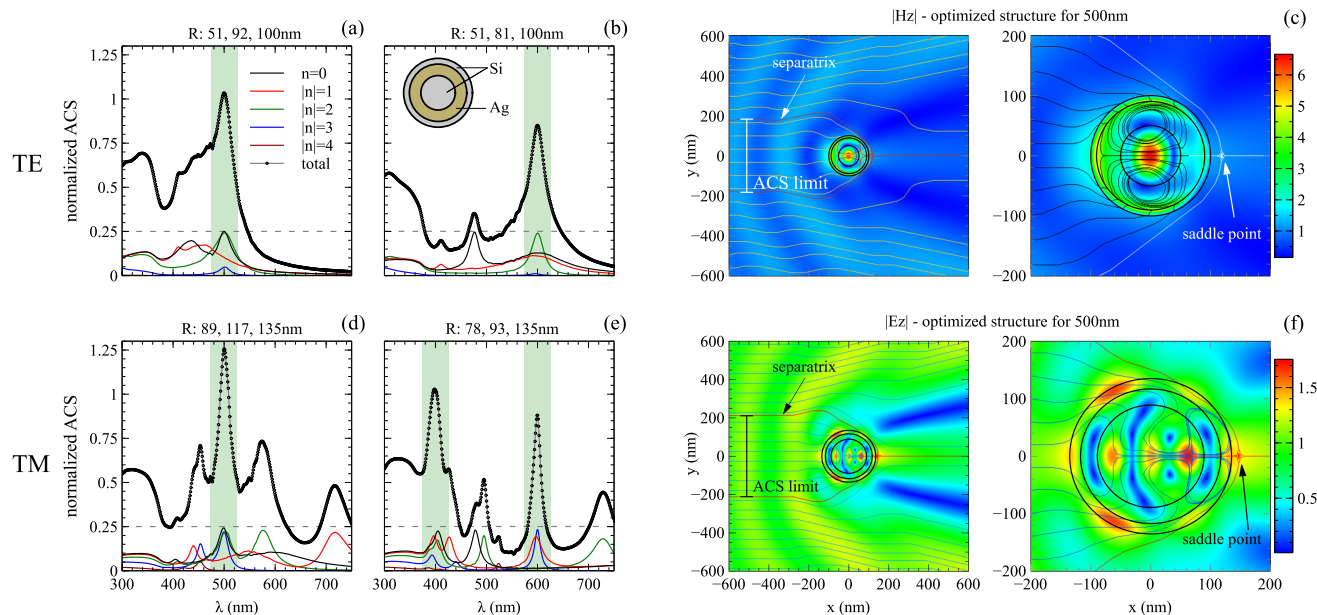


Fig. 3 Optimized nanowires for multiband absorption for both polarizations for Si-Ag-Si configuration. Figures (a, b, d and e) correspond to different multilayer structures with the radii of the layers shown above panels. Outer radius is fixed at 100 nm and 135 nm for TE and TM polarizations, respectively (the same as in Fig. 2). (c) and (f) demonstrate field profiles and energy flow lines. The light is trapped and absorbed in the semiconductor material.

length, can be found as:^{40,41} $\sigma^s = \frac{2\lambda}{\pi} \sum_{n=-\infty}^{+\infty} |\rho_n^{L+1}|^2$. The extinction cross-section is defined as a ratio of the sum of the total scattered and absorbed powers per unit length to the incident energy flux per unit length, and it can be expressed as:^{40,41} $\sigma^e = \frac{2\lambda}{\pi} \sum_{n=-\infty}^{+\infty} \text{Re}\{\rho_n^{L+1}\}$. Therefore, ACS for each mode is found as $\sigma_n^a = \sigma_n^e - \sigma_n^s$. We introduce a normalized cross-section, $\hat{\sigma} = \frac{\pi}{2\lambda} \sigma$. It can be shown that the single mode limit of $\hat{\sigma}_n^s$ and $\hat{\sigma}_n^e$ is equal to unity and $\hat{\sigma}_n^a$ is limited by 0.25, similar to spherical nanostructures.⁴³ To overcome this limit, we propose to overlap several resonances at a given frequency, so that the combined absorption of multiple resonances is larger than that for a single mode. We call such regime as superabsorption. Clearly, this only becomes possible, when absorption of each of the involved resonances is high enough, and we show below, that by using numerical optimization it becomes possible to design structures that outperform single resonance limit at any desired wavelength within visible frequency range.

To have a better understanding of spectral distribution of σ^a , ACS of solid silicon and silver nanowires is analyzed in Fig. 2 for TE polarization and similarly this can be done for TM polarization. The results for a solid silicon nanowire in Fig. 2(a) suggest that the absorption resonances of different modes are spread over a wide spectral range, and the total ACS is almost limited to the summation of positive and negative orders of a single harmonic. Figure 2(b) shows that in a solid

silver nanowire, the absorption resonances are concentrated near the plasmonic resonance wavelength, and ACS is rapidly decreasing to the values under the single-mode limit for the rest of the spectrum. Spectra with similar features characterize solid nanowires for TM polarization.

As the next step, we analyze multilayer structures for the example of Si-Ag-Si geometry, for both TE and TM polarizations. The key strategy to enhance the absorption efficiency of a nanostructure is to increase the number of supported resonances while maintaining the same particle size,^{32,44} which also provides a meaningful comparison of the ACS in multilayer structure with that of the solid nanowires. The results for the absorption enhancement by multilayer nanowires are demonstrated in Fig. 3. The results for two different nanowires are presented in Fig. 3 for both polarizations, showing overlapping of absorption resonances of different modes.

Figure 3(b) demonstrates a superabsorption effect due to the overlap of the resonances of four different modes at $\lambda = 600$ nm. By using the optimization techniques, it is also possible to design structures that demonstrate the enhanced absorption for several wavelengths. For example, Fig. 3(e) also shows a specific configuration for which simultaneous superabsorption is obtained for two different wavelengths within the visible range.

By comparing Figs. 2 and 3, we notice that we can obtain single-band or multi-band enhanced absorption at wave-

lengths for which none of the solid nanowires show considerable absorption. Figures 3 also demonstrates a possibility of tuning the superabsorption effect in multilayer structures to a desired wavelength. Figures 3(a, b) for TE polarization and Figs. 3(d, e) for TM polarization are for two different multilayer structures with different layer thickness that can demonstrate the superabsorption effect in different parts of the spectrum, while having a fixed external radius.

Figures 3(c, f) demonstrate the field profile in the structures which are optimized for the superabsorption effect at $\lambda = 500$ nm. The profiles show trapping of light in semiconductor layers, which for the example of TM polarization (Fig. 3(f)) leads to 78% of the enhanced absorption to occur in silicon.

The energy flow streamlines show how the nanowires absorb light, effectively collecting light from the area that is larger than the geometrical cross-section of the nanowire. To have an in-depth interpretation, we calculate the Poynting vector singular points known as saddle points^{45,46}. The energy flowing close to this points define the separatrices, which in this case have the meaning of the interfaces separating the regions where the energy flows into the nanowire and the region where the energy flows past the nanoparticle. The separatrices are highlighted in Figs. 3(c, f). Some part of the energy propagating into the nanowires may escape out again without being absorbed. Therefore, the separatrices indicate the upper limit for the absorption cross-section. In the presented nanowires designed for superabsorption at $\lambda = 500$ nm for TE and TM polarizations, ACS is equal to $\sigma_{TE}^a = \hat{\sigma}_{TE}^a \times 2\lambda/\pi = 1.0344 \times 2\lambda/\pi = 330$ nm and $\sigma_{TM}^a = 1.2569 \times 2\lambda/\pi = 400$ nm, respectively. Comparison of these results with the ACS limit shown in Figs. 3(c, f), suggests that almost maximum possible energy is absorbed by the nanowires (more than 90% and 94%, for TE and TM polarizations, respectively). Relatively strong absorption of both TE and TM waves in the cylindrical structures can be achieved by compromising absorption of each individual polarization. We expect that less polarization sensitive effect can be achieved in a more symmetric structure such as sphere.

As we have demonstrated, the superabsorption occurs when we overlap several resonances in the structure. We can reasonably expect that these resonances can be of different character, such as electric as in plasmonic or magnetic as in all-dielectric structures. In addition to overlapping the resonances, we need to ensure that these modes should be well absorbing. In general, the absorption of the particle in resonance depends on the resonant mode structure, and there are optimal values of material loss parameters that provide best absorption. In all-dielectric structures, absorption in dielectrics may be sufficient in order to provide efficient absorption, and presence of metals are not a necessary condition for creating a super-absorber. This is demonstrated in Fig.4 by analyzing the absorption properties of an all-dielectric multilayer nanowire with Si-

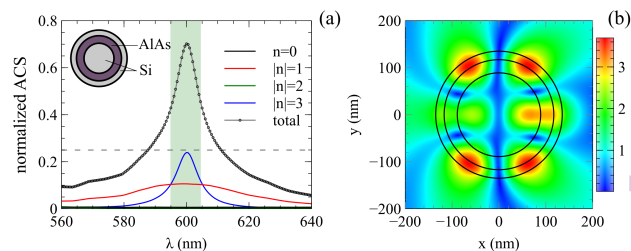


Fig. 4 (a) Superabsorption effect tuned at $\lambda = 600$ nm in an all-dielectric nanowire made of Si and AlAs layers (TM polarization). The radii are 75, 115 and 135 nm. (b) The electric field profile and the enhanced absorption of light in the silicon layers due to the losslessness of AlAs in 600 nm.

AlAs-Si layers in which the superabsorption wavelength is tuned to $\lambda = 600$ nm. The enhanced absorption is due to absorption of light in silicon, as AlAs is practically lossless in this range of frequency⁴⁷.

Finally, we note that applying a similar approach to several scattering resonances in a multilayer nanostructure can lead to the superscattering effect,^{37,48–51} where the optimal conditions are different due to distinctive near- and far-field resonances.⁵²

In conclusion, we have studied the superabsorption in multilayer nanowires achieved by overlapping absorption resonances of different modes of cylindrical structures. We have compared the results for solid nanowires to multilayer structures of the same size and revealed that by carefully designing multilayer structures, it is possible to achieve superabsorption of light even for the wavelengths that none of the similar solid nanostructures have considerable absorption. We have calculated singular points of the energy flow, which allow us to explain the origin of the superabsorption effect in such structures. Possibility to precisely tune the superabsorption effect is also demonstrated by modifying only the size parameters in both TE and TM polarizations. The presented approach can be used for both enhancement and suppression of ACS, similar to the scattering enhancement (superscattering effect) and suppression (invisibility cloaking) by overlapping the resonances or minima of the cross-sections of different modes respectively.

This work was supported by the Australian Research Council.

References

- 1 G. D. Scholes, G. R. Fleming, A. Olaya-Castro, and R. Grondelle. Lessons from nature about solar light harvesting. *Nature Chem.*, 3:763–774, 2011.

- 2 H. Noh, Y. Chong, A. Stone, and H. Cao. Perfect coupling of light to surface plasmons by coherent absorption. *Phys. Rev. Lett.*, 108:186805, 2012.
- 3 J. Zhang, K. F. MacDonald, and N. I. Zheludev. Controlling light-with-light without nonlinearity. *Light: Sci. App.*, 1:e18, 2012.
- 4 M. Brehm, T. Taubner, R. Hillenbrand, and F. Keilmann. Infrared spectroscopic mapping of single nanoparticles and viruses at nanoscale resolution. *Nano Lett.*, 6:1307–1310, 2006.
- 5 I. El-Sayed, X. Huang, and M. El-Sayed. Selective laser photo-thermal therapy of epithelial carcinoma using anti-egfr antibody conjugated gold nanoparticles. *Cancer Lett.*, 239:129–135, 2006.
- 6 P. Jain, I. El-Sayed, and M. El-Sayed. Au nanoparticles target cancer. *Nanotoday*, 2:18–29, 2007.
- 7 K. Jain. Applications of nanobiotechnology in clinical diagnostics. *Clinical Chem.*, 53:2002–9, 2007.
- 8 B. Kang, M. Mackey, and M. El-Sayed. Nuclear targeting of gold nanoparticles in cancer cells induces dna damage, causing cytokinesis arrest and apoptosis. *J. Am. Chem. Soc.*, 132:1517–1519, 2010.
- 9 K. Higgins, S. Benjamin, T. Stace, G. Milburn, B. Lovett, and E. Gauger. Superabsorption of light via quantum engineering. *Nat. Comm.*, 5:4705, 2014.
- 10 T. Hasobe, H. Imahori, P. Kamat, and S. Fukuzumi. Quaternary self-organization of porphyrin and fullerene units by clusterization with gold nanoparticles on sno2 electrodes for organic solar cells. *J. Am. Chem. Soc.*, 125:14962–14963, 2003.
- 11 K. Nakayama, K. Tanabe, and H. Atwater. Plasmonic nanoparticle enhanced light absorption in gaas solar cells. *Appl. Phys. Lett.*, 93:121904, 2008.
- 12 J. Grandidier, D. Callahan, J. Munday, and H. Atwater. Light absorption enhancement in thin-film solar cells using whispering gallery modes in dielectric nanospheres. *Adv. Mat.*, 23:1272–1276, 2011.
- 13 G. E. Jonsson, H. Fredriksson, R. Sellappan, and D. Chakarov. Nanostructures for enhanced light absorption in solar energy devices. *Int. J. Photoenergy*, 2011:939807, 2011.
- 14 J. Warnan, Y. Pellegrin, E. Blart, and F. Odobel. Supramolecular light harvesting antennas to enhance absorption cross-section in dye-sensitized solar cells. *Chem. Commun.*, 48:675–677, 2012.
- 15 T. V. Teperik, F. J. Garcia de Abajo, A. G. Borisov, M. Abdelsalam, P. N. Bartlett, Y. Sugawara, and J. J. Baumberg. Omnidirectional absorption in nanostructured metal surfaces. *Nature Photonics*, 2:299–301, 2008.
- 16 Q. Han, L. Jin, Y. Fu, and W. Yu. Si substrate-based metamaterials for ultrabroadband perfect absorption in visible regime. *J. Nanomaterials*, 2014:893202, 2014.
- 17 Q. Han, Y. Fu, L. Jin, J. Zhao, Z. Xu, F. Fang, J. Gao, and W. Yu. Germanium nanopyramid arrays showing near-100% visible regime. *Nano Res.*, page Accepted, 2015.
- 18 Y. Radi, C. R. Simovski, and S. A. Tretyakov. Thin perfect absorbers for electromagnetic waves: Theory, design, and realizations. *Phys. Rev. App.*, 3:037001, 2015.
- 19 Y. Radi, V. Asadchy, S. Kosulnikov, M. Omelyanovich, D. Morits, A. Osipov, C. Simovski, and S. Tretyakov. Full light absorption in single arrays of spherical nanoparticles. *ACS Photonics*, page Accepted, 2015.
- 20 V. Grigoriev, N. Bonod, J. Wenger, and B. Stout. Optimizing nanoparticle designs for ideal absorption of light. *ACS Photonics*, 2:263–270, 2015.
- 21 J. Zhu, Z. Yu, G. Burkhard, C. Hsu, S. Connor, Y. Xu, Q. Wang, M. McGehee, S. Fan and Y. Cui. Optical absorption enhancement in amorphous silicon nanowire and nanocone arrays. *Nano Lett.*, 9:279–282, 2009.
- 22 S. Diedenhofen, O. Janssen, G. Grzela, E. Bakkers, and J. Rivas. Strong geometrical dependence of the absorption of light in arrays of semiconductor nanowires. *ACS Nano*, 5:2316–2323, 2011.
- 23 N. Anttu, A. Abrand, D. Asoli, M. Heurlin, I. Aberg, L. Samuelson, and M. Borgstrom. Absorption of light in in-plane nanowire arrays. *Nano Research*, 7:816–823, 2014.
- 24 Y. Yu, V. E. Ferry, A. P. Alivisatos, and L. Cao. Dielectric coreshell optical antennas for strong solar absorption enhancement. *Nano Lett.*, 12:3674–3681, 2012.
- 25 C. Guclu, S. Campione, and F. Capolino. Hyperbolic metamaterial as super absorber for scattered fields generated at its surface. *Phys. Rev. B*, 86:205130, 2012.
- 26 J. Liu, G. V. Naik, S. Ishii, C. DeVault, A. Boltasseva, V. M. Shalaev, and E. Narimanov. Optical absorption of hyperbolic metamaterial with stochastic surfaces. *Opt. Express*, 22:8893–8901, 2014.
- 27 D. Ji, H. Song, X. Zeng, H. Hu, K. Liu, N. Zhang, and Q. Gan. Broadband absorption engineering of hyperbolic metafilm patterns. *Scientific Rep.*, 4:4498, 2014.
- 28 J. Cesario, R. Quidant, G. Badenes, and S. Enoch. Electromagnetic coupling between a metal nanoparticle grating and a metallic surface. *Opt. Letters*, 30:3404–3406, 2005.
- 29 K. Aydin, V. E. Ferry, R. M. Briggs, and H. A. Atwater. Broadband polarization-independent resonant light absorption using ultrathin plasmonic super absorbers. *Nature Comm.*, 2:517, 2011.
- 30 T. Sondergaard, S. Novikov, T. Holmgaard, R. Eriksen, J. Beermann, Z. Han, K. Pedersen, and S. Bozhevolnyi. Plasmonic black gold by adiabatic nanofocusing and absorption of light in ultra-sharp convex grooves. *Nat. Comm.*, 3:969, 2012.
- 31 D. R. Abujetas, R. Paniagua-Dominguez, and

- J. A. Sanchez-Gil. Unraveling the janus role of mie resonances and leaky/guided modes in semiconductor nanowire absorption for enhanced light harvesting. *ACS Photonics*, page Accepted, 2015.
- 32 S. Mann and E. Garnett. Extreme light absorption in thin semiconductor films wrapped around metal nanowires. *Nano Lett.*, 13:3173–3178, 2013.
- 33 S. Ramadurgam, T. Lin, and C. Yang. Aluminum plasmonics for enhanced visible light absorption and high efficiency water splitting in core-multishell nanowire photoelectrodes with ultrathin hematite shells. *Nano Lett.*, 14:4517–4522, 2014.
- 34 E. Palik. *Handbook of Optical Constants of Solids*. Academic Press, 1997.
- 35 D. Aspnes and A. Studna. Dielectric functions and optical parameters of si, ge, gap, gaas, gasb, inp, inas, and insb from 1.5 to 6.0 ev. *Phys. Rev. B*, 27:985, 1983.
- 36 C. Bohren, D. Huffman. *Absorption and Scattering of Light by Small Particles*. J. Wiley, 1983.
- 37 A. Mirzaei, A. Miroshnichenko, I. Shadrivov, and Y. Kivshar. Superscattering of light optimized by a genetic algorithm. *Appl. Phys. Lett.*, 105:011109, 2014.
- 38 A. Mirzaei, and A. Miroshnichenko. Electric and magnetic hotspots in dielectric nanowire dimers. *Nanoscale*, 7:5963–8, 2015.
- 39 A. Mirzaei, A. Miroshnichenko, I. Shadrivov, and Y. Kivshar. All-dielectric multilayer cylindrical structures for invisibility cloaking. *Sci. Rep.*, 5:9574, 2015.
- 40 C. A. Balanis. *Advanced Engineering Electromagnetics*. Wiley, 1989.
- 41 L. Schachter. *Beam-Wave Interaction in Periodic and Quasi-Periodic Structures*. Springer, 2011.
- 42 U. Kreibig. Electronic properties of small silver particles: the optical constants and their temperature dependence. *J. Phys. F: Metal Phys.*, 4:999–1014, 1974.
- 43 M. Tribelsky. Anomalous light absorption by small particles. *EPL*, 94:14004, 2011.
- 44 G. Grzela, R. Paniagua-Domnguez, T. Barten, Y. Fontana, J. A. Snchez-Gil, and J. G. Rivas. Nanowire antenna emission. *Nano Lett.*, 12:5481–5486, 2012.
- 45 B. Luk'yanchuk and V. Ternovsky. Light scattering by a thin wire with a surface-plasmon resonance: Bifurcations of the poynting vector field. *Phys. Rev. B*, 73:235432, 2006.
- 46 B. Luk'yanchuk, A. Miroshnichenko, and Y. Kivshar. Fano resonances and topological optics: an interplay of far- and near-field interference phenomena. *J. Opt.*, 15:073001, 2013.
- 47 R. Fern and A. Onton. Refractive index of alas. *J. Appl. Phys.*, 42:3499–3500, 1971.
- 48 Z. Ruan and S. Fan. Superscattering of light from sub-wavelength nanostructure. *Phys. Rev. Lett.*, 105:013901, 2010.
- 49 Z. Ruan and S. Fan. Design of subwavelength superscattering nanospheres. *Appl. Phys. Lett.*, 98:043101, 2011.
- 50 A. Mirzaei, I. Shadrivov, A. Miroshnichenko, and Y. Kivshar. Cloaking and enhanced scattering of core-shell plasmonic nanowires. *Opt. Express*, 21:10454–10459, 2013.
- 51 A. Mirzaei, A. Miroshnichenko, N. Zharova, and I. Shadrivov. Light scattering by nonlinear cylindrical multilayer structures. *JOSA B*, 31:1595–1599, 2014.
- 52 Andrey E. Miroshnichenko. Off-resonance field enhancement by spherical nanoshells. *Phys. Rev. A*, 81:053818, May 2010.

Graphical abstract:

Multilayer dielectric and hybrid nanowires make it possible to achieve enhanced, frequency-selective, multiband absorption of light.

